

High Coercive RE-Fe-B Powders Recycled *via* HD and HDDR Process from Waste Magnets

Tae-Sung Noh^{1,2}, Hee-Ryoung Cha¹, Yang-Do Kim^{2*}, and Jung-Goo Lee^{1*}

¹Department of Magnetic Materials, Korea Institute of Materials Science, 797 Changwondaero, Changwon, 51508, Republic of Korea

²Department of Materials Science and Engineering, Pusan National University, 2, Busandaehak-ro 63beon-gil, Geumjeong-gu, Republic of Korea

(Received 10 May 2022, Received in final form 10 June 2022, Accepted 10 June 2022)

In order to fabricate high-coercivity hard magnetic RE-Fe-B powders from the waste bulk magnets, the hydrogen decrepitation (HD) and hydrogenation-disproportionation-desorption-recombination (HDDR) processes were employed to the waste RE-Fe-B magnets. The optimum HD and HDDR conditions for the waste RE-Fe-B magnets were established through the systematic investigation on the effect of HD and HDDR treatment temperature on the magnetic and microstructural properties of final recycled powders. We found that the waste magnets were crushed into the flakes with a uniform size distribution when the HD treatment was carried at 200 °C. By applying the HDDR process to the HD treated flakes at 920 °C, high coercivity of 11.2 kOe could be achieved in the recycled RE-Fe-B HDDR powders. Based on the results from the microstructural characterization, the underlying reasons for the magnetic and microstructural changes of the recycled powders as a function of the HD and HDDR treatment temperature is discussed in detail.

Keywords : Nd-Fe-B magnets, recycling, hydrogen decrepitation (HD), hydrogenation-disproportionation-desorption-recombination (HDDR)

1. Introduction

RE-Fe-B-based sintered magnets have been widely used in various industries due to its outstanding hard magnetic properties. Recently, demand for high performance RE-Fe-B magnets in applications such as electric vehicles (EV) and wind turbines is increasing rapidly [1]. However, the increasing demand and China's monopoly on supply of rare-earth (RE) metals have led to a sharp rise in the price of RE resources. For the stability of supply and price of RE metals, there is a strong demand for recycling of waste RE-Fe-B magnets generated from the end-of-life parts [1, 2]. There have been many attempts to develop recycling technology of RE-Fe-B magnets using various processes, such as hydrogen decrepitation (HD) [3, 4], hydrometallurgical/pyrometallurgical process [5, 6], chemical vapor transport [7], liquid metal extraction [8], etc. Among them, the HD process seems to be the most promising

method in recycling of the waste RE-Fe-B magnets because it is simple, cost-effective, environmental-friendly, and easy to obtain magnetically anisotropic flakes [2, 9]. However, the coercivity achieved in the recycled HD powders is lower than expected, which is one of the critical obstacles for recycling of the waste RE-Fe-B magnets [9, 10]. It is well known that the hydrogenation-disproportionation-desorption-recombination (HDDR) process is an effective method to fabricate high coercivity RE-Fe-B powders comprising ultra-fine grains [11, 12]. In addition, by controlling the processing conditions, such as hydrogen pressure in the hydrogenation-disproportionation stage and dehydrogenation speeds in the desorption-recombination stage, the magnetic/crystallographic anisotropy of the powders can be controlled [13, 14]. The anisotropic HDDR powder could be used for bonded magnets or fully dense sintered magnets by hot-press [15], whereas isotropic HDDR powder could be used for hot-deformed magnets [16]. For this reason, the HDDR process has attracted much attention in the recycling of the waste RE-Fe-B magnets [11, 12, 17, 18]. However, the process has not yet been optimized for waste RE-Fe-B magnets with high oxygen content.

©The Korean Magnetism Society. All rights reserved.

*Co-corresponding author: Tel: +82-51-510-2478

e-mail: yangdo@pusan.ac.kr

Tel: +82-55-280-3606

e-mail: jglee36@kims.re.kr

In this study, in order to establish the optimum process for recycling of the waste RE-Fe-B magnets, we systematically investigated HD behavior at various temperature and effect of HDDR temperature on the magnetic properties and microstructure using waste RE-Fe-B magnets for high performance HDDR powders.

2. Experimental Procedure

Waste RE-Fe-B magnets with nominal composition of $Dy_{1.4}Nd_{21.8}Pr_{6.7}Fe_{bar}B_{0.9}M_{2.0}$ ($M=Co, Al, Cu, Ga, \text{ and } Nb$) (wt.%) was used as starting material. The initial magnets were hydrogen decrepitated at 30 °C, 100 °C, 200 °C, and 300 °C under 1.5 atm of hydrogen pressure for 1 hours. The samples were dehydrogenated at 500 °C under vacuum (rotary pump, $\sim 10^{-2}$ torr). After the HD process, pulverized flakes were heated up to 810 °C, 840 °C, 880 °C, 920 °C, and 940 °C under argon atmosphere. For the hydrogenation disproportionation reaction, argon gas was removed to 0.8 atm, and then hydrogen gas of 300 cc/min was flowed while maintaining furnace pressure of 1.1 atm for 2 hours at each processing temperature. In the desorption recombination stage, the flakes exposed to a mixture of hydrogen and argon gas ($P_{H_2} = 0.1$ atm) without changing the temperature. After a 10 min hold, the furnace was evacuated to 10^{-2} torr for 25 min using rotary pump. Finally, the furnace was quenched using argon gas down to room temperature. The schematic diagram of HD and HDDR process are shown in Fig. 1. The size of HD treated flake was measured by sieving with different mesh number sieves (7, 18, 35, 50, 120,

230, 600 mesh number). The fracture surface images and backscattered electron (BSE) images were taken using field emission scanning electron microscopy (FE-SEM; JSM-7001F; Jeol). The magnetic properties of the HDDR treated powders were measured using a vibrating sample magnetometer (VSM; VSM 7407; LakeShore) after pre-magnetizing with a pulsed magnetic field of 6 T. For VSM measurement, HDDR treated flakes were crushed into 200-300 μm and fixed with paraffin wax under a magnetic field of 1.2 T.

3. Results and Discussion

Figure 2 shows the microstructure of initial magnets. The average grain size of initial magnets is approximately 5 μm with inhomogeneous grain size distribution as shown in Fig. 2(a). BSE mode was used to observe the phase distribution [Fig. 2(b)], the gray and bright contrast can be assigned to the $RE_2Fe_{14}B$ matrix phase and RE-rich phase, respectively. The RE-rich phase existed at the grain boundary and aggregated at the triple junction area. The composition and microstructure of these initial magnets can affect the magnetic properties of the HDDR powder. The homogeneously distributed RE-rich phase of initial alloy could increase the coercivity of the final HDDR treated powders by forming the homogeneous RE-rich gain boundary of HDDR treated powders [19].

To pulverize the initial magnets, HD process was employed. Generally, HD process is used as a pre-treatment step for pulverizing the alloy into fine powder in the conventional production of RE-Fe-B sintered magnets.

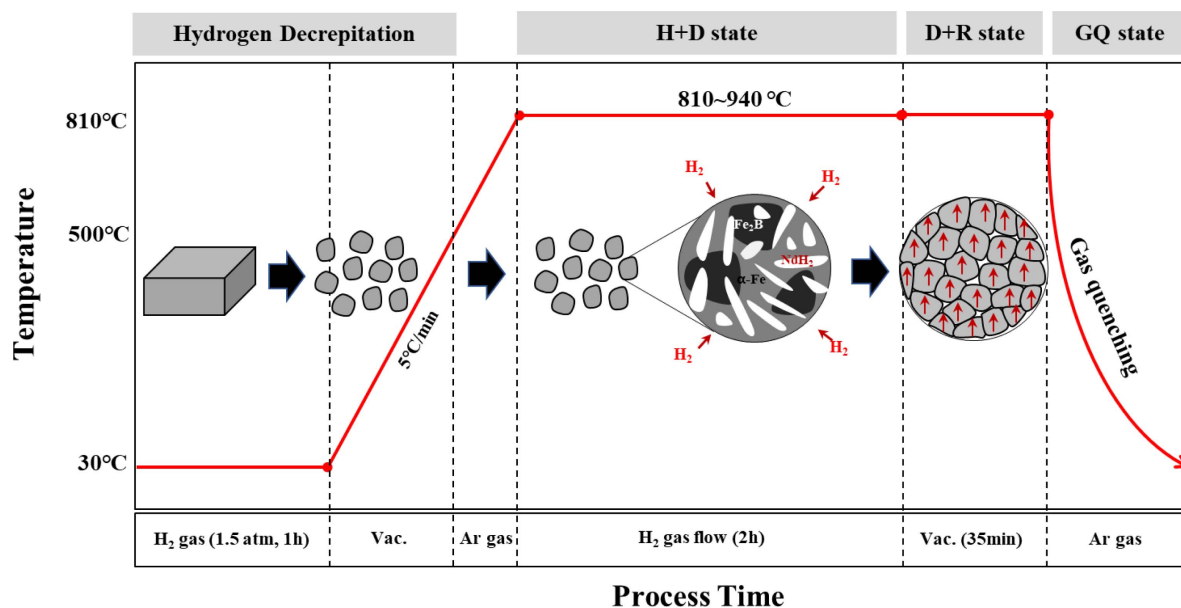


Fig. 1. (Color online) Schematic diagram of the HDDR process employed in the study.

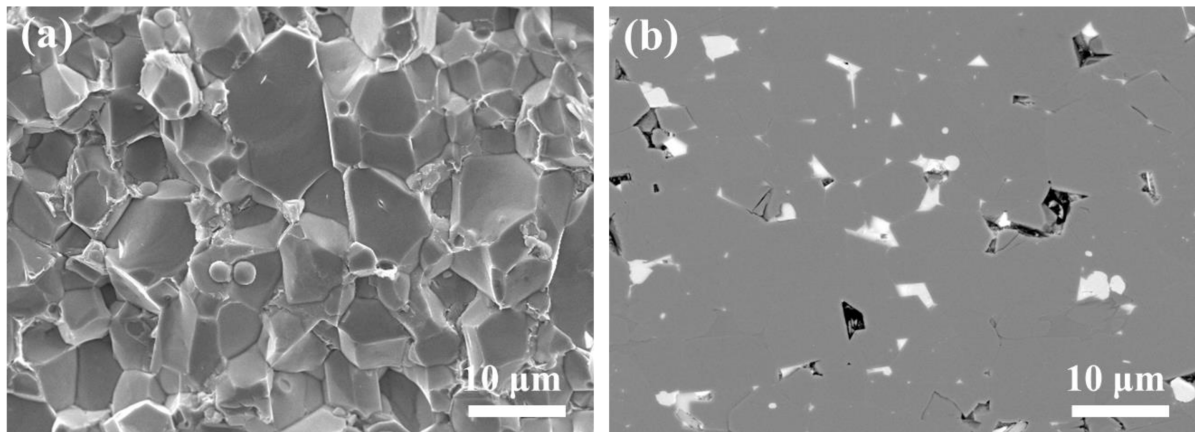


Fig. 2. (a) Fracture surface and (b) backscattered electron image of initial magnets.

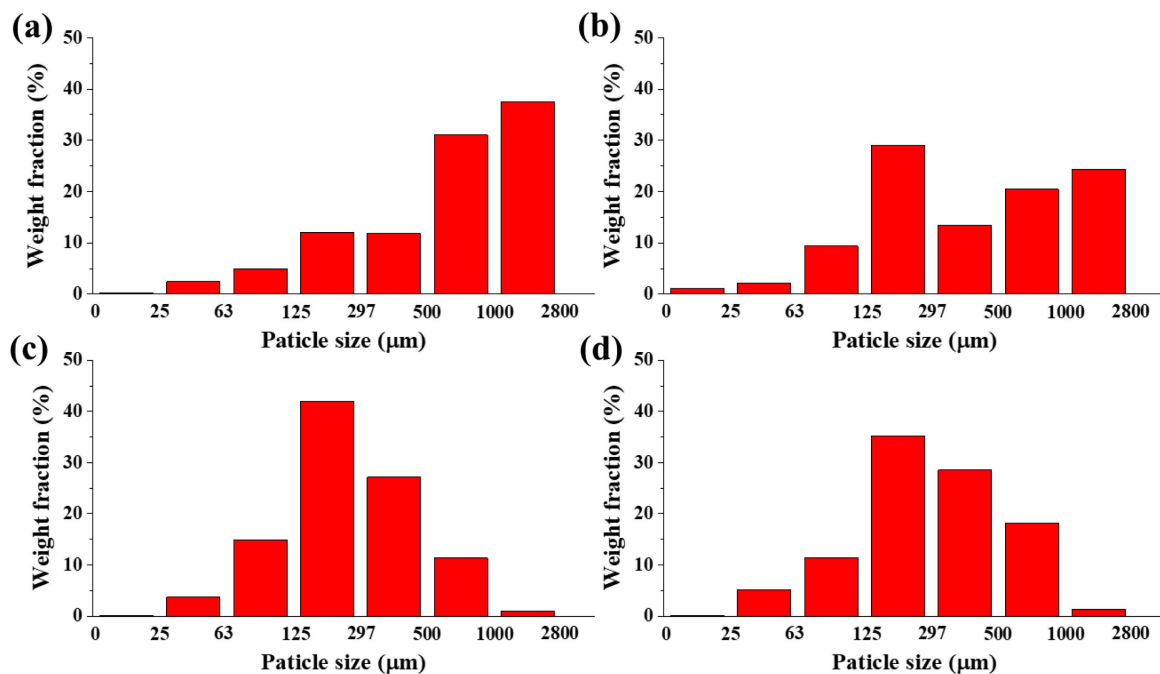


Fig. 3. (Color online) Particle-size histograms of HD treated flakes as function of HD temperature. (a) 30 °C, (b) 100 °C, (c) 200 °C, and (d) 300 °C.

During the hydrogenation, both the $\text{RE}_2\text{Fe}_{14}\text{B}$ matrix phase and RE-rich phase in RE-Fe-B alloys absorb hydrogen, thereby expanding their volume. The hydrogen preferentially reacts with the RE-rich phase, causing shear stress due to volume expansion and consequently the cracks between the $\text{RE}_2\text{Fe}_{14}\text{B}$ matrix phase and RE-rich phase are formed [20]. Figure 3 shows powder size distribution after HD process at various temperature. In order to prevent the phase decomposition of $\text{RE}_2\text{Fe}_{14}\text{B}$ hydride into the REH_x , $\alpha\text{-Fe}$, and Fe_2B at ~ 650 °C, dehydrogenation of the matrix phase before HDDR process at temperature below 650 °C was carried out [21]. The HD treated magnets at 30 °C, 100 °C, 200 °C, and

300 °C were pulverized into small flakes less than 2.8 mm. It can be clearly seen in Fig. 3 that the size of flakes after HD treatment tends to be smaller as the HD temperature increases from 30 to 200 °C. However, the size of the flakes increased again as the HD temperature increased from 200 to 300 °C, as shown in Fig. 3. As mentioned above, at room temperature, the magnets were pulverized into flakes due to the volume change of the RE-rich phase by hydrogenation reaction. However, during the HD treatment at 200 °C, differences in thermal expansion coefficient between matrix and RE-rich phase could induce the additional micro-cracks in the magnets [22, 23]. Regarding the thermal expansion of RE-Fe-B

magnets, the RE-rich phase always expands with increasing temperature. However, in the case of matrix, the thermal shrink occurs along the a-axis while the thermal expansion occurs along the c-axis as the temperature increases to Curie temperature (312 °C) [22]. This is because the change in spontaneous magnetostriction of the $\text{RE}_2\text{Fe}_{14}\text{B}$ phase occurs along the a-axis at around their curie temperature [22]. Therefore, it is expected that the difference in the volume change between the matrix and RE-rich phase is larger at around 300 °C, thereby forming micro-cracks, which can be a diffusion path of hydrogen during the HD treatment. However, the rapid diffusion of hydrogen due to internal micro-cracks could causes the hydrogenation of the matrix phase and the RE-rich phase to occur simultaneously, and consequently, the difference in volume expansion by hydrogenation could be reduced. Therefore, moderated micro-cracks by thermal expansion before hydrogenation is required to making a fine and uniformly sized flakes, and the most homogeneous powder was obtained by HD treatment at 200 °C.

The HD-treated powder can be used in various applications such as HDDR process, re-sintering, polymer bonding, etc [3, 4]. For the HDDR process, HD-treated flakes at 30 °C with a relatively large size were used to minimize the deterioration of magnetic properties due to surface oxidation, which could create soft magnetic phase such as $\alpha\text{-Fe}$ during the HDDR process [11, 24]. After HD process, the flakes were HDDR treated at 810, 840, 880, 920, and 940 °C. Figure 4 shows the dependence of coercivity, remanence and maximum energy product of HDDR treated powders. the coercivity of powders were gradually increased with increasing HDDR temperature to 920 °C. However, at the 940 °C, the coercivity was sharply decreased. As mentioned above, the coercivity of magnets closely related to their microstructure, such as grain size and grain boundary phase. The fracture surface and BSE image of HDDR powders are shown in Fig. 5. The average grain size of HDDR powder were increased with increasing HDDR temperature. The HDDR powders treated at 810 °C has relatively small grain size approximately 250 nm, including a large fractured region about 1 μm with discontinuous grain boundaries (shown by arrows in Fig. 5(a)) where the grains shape is not clear. The region with discontinuous grain boundaries could be a reason for low coercivity of HDDR treated powders because the grains in such area are exchange coupled. The HDDR temperature of 810 °C seems to be not enough to form the RE-rich grain boundary phase [21, 25]. In the case of the grains of the HDDR powders treated at 920 °C, the $\text{RE}_2\text{Fe}_{14}\text{B}$ phase with a size of approximately 500 nm were uniformly formed after the

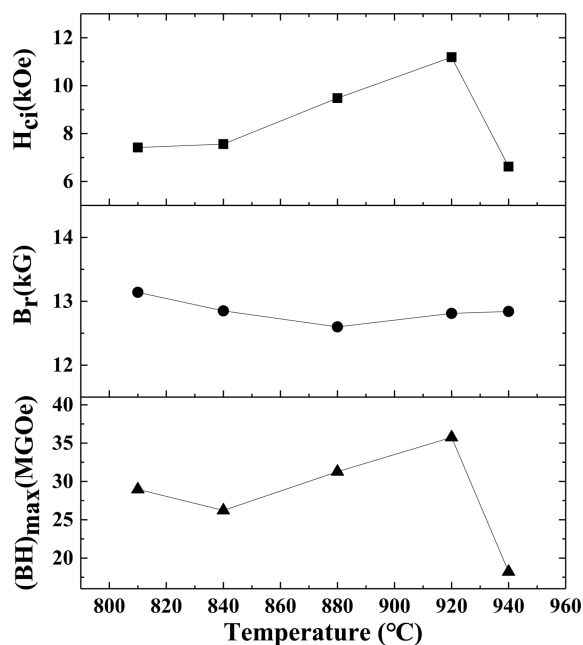


Fig. 4. Dependence of H_{ci} , B_r and $(BH)_{max}$ of HDDR treated powders on HDDR temperature.

HDDR treatment, as shown in Fig. 5(c). In addition, as shown in Fig. 5(d), the RE-rich grain boundary phase was also homogeneously distributed. Therefore, the highest coercivity could be achieved in the recycled HDDR powders when the HDDR treatment was carried out at 920 °C, as shown in Fig. 4. The coercivity of HDDR treated powder was rapidly decreased with increasing process temperature to 940 °C. For the powders HDDR treated at 940 °C, it can be seen from Fig. 5(e) and (f) that the distribution of the grain size and the RE-rich grain boundary phase were considerably inhomogeneous. Since the absence of a non-magnetic grain boundary phase in the magnetic powder causes reverse magnetic domain nucleation and coupling between neighboring grains, which causes a decrease in coercivity. Therefore, formation of homogeneous grain boundary phase is important for high coercivity. In addition, large grains were observed in some areas, as shown in the inset image in Fig. 5(e). In the Nd-Fe-B ternary system, it has been reported that recombination occurs at a high temperature around 950 °C under the hydrogen atmosphere [21]. This indicates the possibility that the disproportionation was difficult to completely occur at a temperature at 940 °C. Thus, it is expected that some unreacted large grains were observed in HDDR treated powder at 940 °C.

The remanence was slightly decreased with increasing HDDR temperature to 880 °C and increased again with increasing HDDR temperature. It may be because the processing temperature could change the hydrogenation-

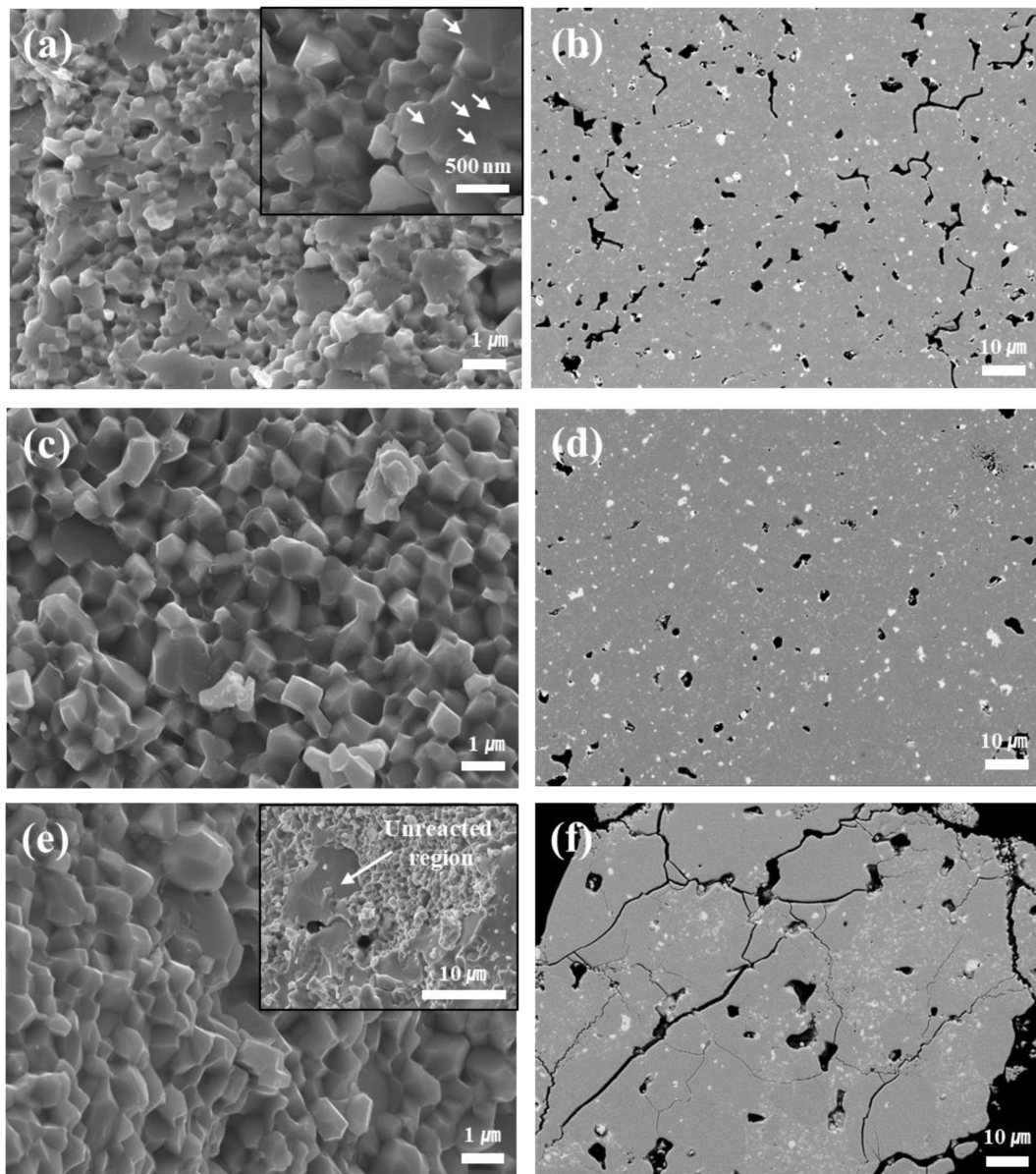


Fig. 5. (a, c, e) Fracture surface and (b, d, e) backscattered electron images of HDDR powder treated at (a,b) 810 °C, (c, d) 920 °C, and (e, f) 940 °C. Insets in (a) and (e) are high and low magnified images, respectively.

disproportionation and desorption-recombination speed. It is reported that low hydrogen pressure about 0.3 atm in hydrogenation-disproportionation stage and slow desorption recombination speed could induced the improved alignment of grains c-axis in HDDR treated powder [13, 14].

Regarding the maximum energy product, it is well known that the maximum energy product of a permanent magnet depends on the remanence value if the coercivity is numerically greater than remanence and the squareness of the demagnetization curves is good [26]. However, maximum energy product of the fabricated HDDR powders

depends on the coercivity rather than the remanence, as shown in Fig. 4. This is considered to be because not only the coercivity is low, but also the change in the coercivity is larger as function of process temperature compared to the remanence.

The HD and HDDR conditions for recycling of the waste magnets were optimized, and the coercivity, remanence and $(BH)_{\max}$ achieved in this work were 11.2 kOe, 12.8 kG and 35.7 MGOe, respectively, by HDDR process at 920 °C. Considering the hard magnetic properties of the initial magnets ($H_{ci} = 13.3$ kOe and $B_r = 13.0$ kG), the HD and HDDR process optimized in this

work seems to be effective for recycle of the waste RE-Fe-B magnets. To increase the coercivity of the recycled powders further, the development of the grain boundary diffusion process for nano-grained recycled HDDR powders is essential. After grain boundary diffusion process, it is expected that the coercivity reduced by HDDR process could be recovered or further enhanced than coercivity of initial magnets, forming uniform and continuous non-magnetic grain boundary phase.

4. Conclusion

We have investigated the changes in the HD and HDDR behavior at various temperatures and their influences on magnetic properties and microstructure of the recycled HDDR RE-Fe-B powders. The flake HD treated at 200 °C showed the smallest and uniform size distribution. The moderately created micro-cracks generated by the difference in thermal expansion between matrix phase and RE-rich phase at high temperature could induce uniform hydrogenation to the inside of magnets, resulting in more uniform pulverization. When the HDDR treatment was applied to the HD treated flakes at 920 °C, the highest coercivity with homogeneous RE-rich distribution was achieved. However, the coercivity was still lower than that of the initial magnets, which is thought to be because the surface area increased as the grain size became smaller. Therefore, the grain boundary diffusion process is additionally required for the high coercivity of the nano-grained powders.

Acknowledgments

This work was supported in part by Korea Evaluation Institute of Industrial Technology (KEIT) grant funded by the Korea government (MOTIE) (No. 20010817, 10080382).

References

- [1] Y. Yang, A. Walton, R. Sheridan, K. Güth, R. Gauß, O. Gutfleisch, M. Buchert, B. Steenari, T. Van Gerven, and P. T. Jones, *Journal of Sustainable Metallurgy* **3**, 122 (2017).
- [2] M. Zakotnik, I. R. Harris, and A. J. Williams, *J. Alloys Compounds* **469**, 314 (2009).
- [3] M. Zakotnik, I. R. Harris, and A. J. Williams, *J. Alloys Compounds* **450**, 525 (2008).
- [4] B. Michalski, M. Szymanski, K. Gola, J. Zygmuntowicz, and M. Leonowicz, *J. Magn. Magn. Mater* **548**, 168979 (2022).
- [5] S. Wellens, B. Thijs, and K. Binnemans, *Green Chem.* **14**, 1657 (2012).
- [6] T. Saito, H. Sato, S. Ozawa, J. Yu, and T. Motegi, *J. Alloys Compounds* **353**, 189 (2003).
- [7] M. Itoh, K. Miura, and K. Machida, *J. Alloys Compounds* **477**, 484 (2009).
- [8] T. H. Okabe, O. Takeda, K. Fukuda, and Y. Umetsu, *Materials Transactions* **44**, 798 (2003).
- [9] H. Kwon, I. Jeong, A. Kim, D. Kim, S. Namkung, T. Jang, and D. Lee, *J. Magn. Magn. Mater* **304**, e219 (2006).
- [10] A. Kim, D. Kim, S. Namkung, T. Jang, D. Lee, H. Kwon, and D. Hwang, *IEEE Trans. Magn.* **40**, 2877 (2004).
- [11] A. Lixandru, I. Poenaru, K. Güth, R. Gauß, and O. Gutfleisch, *J. Alloys Compounds* **724**, 51 (2017).
- [12] O. Gutfleisch, K. Güth, T. G. Woodcock, and L. Schultz, *Advanced Energy Materials* **3**, 151 (2013).
- [13] K. Güth, T. Woodcock, L. Schultz, and O. Gutfleisch, *Acta Materialia* **59**, 2029 (2011).
- [14] H. Cha, J. Yu, Y. Baek, H. Kwon, Y. Kim, and J. Lee, *J. Magn.* **19**, 49 (2014).
- [15] A. Ikram, F. Mehmood, R. S. Sheridan, M. Awais, A. Walton, A. Eldosouky, S. Sturm, S. Kobe, and K. Z. Rozman, *Journal of Rare Earths* **38**, 90 (2020).
- [16] H. Cha, J. Yoo, K. Jeon, Y. Baek, H. Kwon, D. Lee, and J. Lee, *IEEE Trans. Magn.* **53**, 1 (2017).
- [17] R. Sheridan, R. Sillitoe, M. Zakotnik, I. Harris, and A. Williams, *J. Magn. Magn. Mater* **324**, 63 (2012).
- [18] R. Sheridan, A. Williams, I. Harris, and A. Walton, *J. Magn. Magn. Mater* **350**, 114 (2014).
- [19] M. Liu, G. B. Han, and R. W. Gao, *Alloys Compounds* **488**, 310 (2009).
- [20] B. Saje, J. Holc, and S. Beseničar, *J. Mater. Sci.* **27**, 2682 (1992).
- [21] D. Book and I. Harris, *J. Alloys Compounds* **221**, 187 (1995).
- [22] C. De Groot and K. de Kort, *J. Appl. Phys.* **85**, 8312 (1999).
- [23] T. Akiya, T. Sasaki, T. Ohkubo, Y. Une, M. Sagawa, H. Kato, and K. Hono, *J. Magn. Magn. Mater* **342**, 4 (2013).
- [24] H. W. Kwon, J. G. Lee, and J. H. Yu, *J. Appl. Phys.* **115**, 17A727 (2014).
- [25] W. Li, T. Ohkubo, K. Hono, T. Nishiuchi, and S. Hiro-sawa, *Appl. Phys. Lett.* **93**, 052505 (2008).
- [26] J. J. Becker, *J. Appl. Phys.* **41**, 1055 (1970).